

## Article

# Impact of Land Use and Land Cover Change on Hydrological Processes in Urban Watersheds: Analysis and Forecasting for Flood Risk Management

Mandip Banjara <sup>1</sup>, Amrit Bhusal <sup>2</sup>, Amrit Babu Ghimire <sup>1</sup>  and Ajay Kalra <sup>1,\*</sup> 

<sup>1</sup> School of Civil, Environmental, and Infrastructure Engineering, Southern Illinois University, 1230 Lincoln Drive, Carbondale, IL 62901-6603, USA; mandip.banjara@siu.edu (M.B.); amrit.ghimire@siu.edu (A.B.G.)

<sup>2</sup> Arcadis U.S., Inc., 7575 Huntington Park Dr. Suite 130, Columbus, OH 43235, USA; amrit.bhusal@arcadis-us.com

\* Correspondence: kalraa@siu.edu

**Abstract:** Land use and land cover (LULC) change is one of the primary contributors to hydrological change in urban watersheds and can potentially influence stream flow and flood volume. Understanding the impacts of LULC change on urban hydrological processes is critical to effective urban water management and minimizing flood risks. In this context, this study aims to determine the impacts of LULC change on hydrological response in a fast transitioning watershed for the predicted years of 2050 and 2080. This research employs the hybrid land use classification technique, Cellular Automata–Markov (CA–Markov) model to predict land use changes, utilizing land use data from 2001, 2013, and 2021. Additionally, it incorporates a calibrated, event-specific hydrologic model known as the Personal Computer Storm Water Management Model (PCSWMM) to assess alterations in hydrological responses for storm events of various magnitudes. The findings indicate a transition of the watershed into an urbanized landscape, replacing the previous dominance of agriculture and forested areas. The initial urban area, constituting 11.6% of the total area in 2021, expands to cover 34.1% and 44.2% of the total area by 2050 and 2080, respectively. Due to the LULC changes, there are increases in peak discharge of 5% and 6.8% and in runoff volume of 8% and 13.3% for the years 2050 and 2080 for a 100-year return period storm event. Yet, the extent of these changes intensifies notably during storm events with lower return periods. This heightened impact is directly attributed to the swift urbanization of the watershed. These results underscore the pressing necessity to regulate LULC change to preserve the hydrological equilibrium.

**Keywords:** LULC; PCSWMM; urbanization; CA–Markov; hydrology; peak discharge; runoff



**Citation:** Banjara, M.; Bhusal, A.; Ghimire, A.B.; Kalra, A. Impact of Land Use and Land Cover Change on Hydrological Processes in Urban Watersheds: Analysis and Forecasting for Flood Risk Management.

*Geosciences* **2024**, *14*, 40. <https://doi.org/10.3390/geosciences14020040>

Academic Editors: Sabina Porfido and Jesus Martinez-Frias

Received: 24 December 2023

Revised: 30 January 2024

Accepted: 31 January 2024

Published: 2 February 2024



**Copyright:** © 2024 by the authors. Licensee MDPI, Basel, Switzerland. This article is an open access article distributed under the terms and conditions of the Creative Commons Attribution (CC BY) license (<https://creativecommons.org/licenses/by/4.0/>).

## 1. Introduction

Land use and land cover (LULC) change refers to changes to the Earth's surface caused by both natural and human-caused factors, such as urbanization [1], deforestation [2], increasing population [3], agricultural activities [4], climatic shifts [5], and more. LULC change and changing climate are the two most important aspects of environmental change which can alter the hydrologic properties of an area through changes in patterns such as infiltration, evaporation, and precipitation [6–8]. Therefore, a special focus has been given in water resources engineering to the study of runoff response to LULC and climate change [9,10].

The issue of urban flooding has increased in recent decades due to the impact of a changing environment [11,12]. The swift rise in population is negatively affecting water resources on both the local and global levels [13,14]. This growth is driving urban expansion to accommodate the escalating population [15]. Urbanization has transformed the natural landscape, replacing green spaces with concrete, asphalt, and other impervious surfaces. The development of roads, residential and commercial buildings alters the runoff coefficient of the catchment and influences the runoff routing process, which in turn increases the peak

stormwater and vulnerabilities to flooding [16]. This effect on hydrological response is dependent on the degree of urbanization within the watershed [17]. Therefore, a limitation on the extent of urban development in catchments can be set if the impacts of urbanization, particularly flooding, are assessed [18]. The effects of LULC change on hydrology can be examined through hydrologic modeling, statistical evaluation, and comparative analysis of experimental catchments [19]. Dwarakish and Ganasri [20] have provided a detailed review of the modeling approaches used to assess the impact of land use change on hydrological response. Out of these methods, hydrological modeling is the one that has been extensively used to assess the impacts on hydrology [21–23]. Hydrologic modeling tools help to predict the impact of changing LULC on flow regimes. There have been studies that have examined changes in the streamflow due to LULC changes [24–27]. Other studies by Setegn et al. [28], Gebremicael et al. [29], and Neupane and Kumar [30] have reported significant changes in the hydrology of watersheds. Studies by Huong and Pathirana [31] and Shanableh et al. [32] have found an increase in stormwater runoff due to the development of impervious surfaces during urbanization. Huong and Pathirana [31] observed a 21% rise in stormwater runoff with a 55% expansion in urban regions using the Storm Water Management Model (SWMM) model, suggesting a notable correlation between urban growth and increased runoff. Getachew and Melesse [24] utilized the Soil and Water Assessment Tool (SWAT) model to analyze the impact of land use conversion in the Angereb watershed, Ethiopia, between 1985 and 2011. Their study revealed a 39% rise in average wet flow and a 46% reduction in dry flow due to the change from forest to agriculture. Conversely, Bahremand et al. [33] discovered a 12% reduction in peak discharge with a 50% increment in forested areas. This signifies that a larger forested area aids in water retention, reducing peak discharge rates. These discoveries highlight the substantial impact of LULC changes on a watershed's hydrological reaction, prompting extensive research for effective water resource management strategies.

However, these studies have focused on existing LULC data, neglecting the incorporation of LULC prediction to assess its impact on hydrological responses. But, for effective water resource management strategies, it is essential to analyze hydrological changes in predicted LULC. This assessment is critical for designing an appropriate drainage system to meet future requirements. There are several models to predict LULC, such as statistical models [34], the Markov chain model [35], logistic regression [36], Cellular Automata (CA) [37], and Artificial Neural Networks (ANNs) [38]. CA is a commonly used method for urban growth modeling [39,40] and has an open structure, which makes it easier to integrate with other models [41]. It also has a strong spatial computing power to simulate spatial variability [42,43]. However, it lacks quantitative aspects and the ability to include driving forces in simulations, making integration with a quantitative model like the Markov chain essential [44]. On the other hand, Markov models excel in capturing long-term patterns but struggle with simulating spatial aspects [45]. Therefore, using only a single model will have simulation limitations. To overcome the limitation of standalone methods, integration of different models can be found in numerous studies [46–50]. Based on a review of the available literature on land use prediction, a combination of CA and Markov is widely used and also addresses the limitations of each [51]. Hence, this research proposes the combination of the CA and Markov models, aiming to enhance simulation accuracy and positively impact the prediction of spatiotemporal scenarios [52]. This integration is supported by Mondal et al. [53], who assert that the combined CA–Markov model demonstrates superior capability in generating accurate spatio-temporal LULC change patterns. This combination also incorporates the probabilistic aspect of the Markov method with the stochastic spatial attributes of the CA method [54]. Therefore, the CA–Markov model has been a widely used model to predict future land use patterns [55–58]. Furthermore, the CA–Markov model's ability to successfully combine geographic information system (GIS) and remote sensing (RS) makes it stand out as a reliable technique for simulating changes in land use across time and space [59].

In contrast to previous research, which usually relies on existing LULC data, this study takes a unique approach. It innovatively employs the CA–Markov model to predict future LULC changes and subsequently utilizes PCSWMM to analyze the hydrological changes. The research hypothesizes that increased urbanization in the watershed will lead to a higher average weighted curve number (CN), resulting in a significant increase in stormwater runoff and volume. This hypothesis underpins the study’s objectives, which are as follows:

- (a) Forecast LULC maps for the years 2050 and 2080 utilizing the CA–Markov model.
- (b) Evaluate the impact of these LULC changes on peak runoff and flood volumes during storm events of varying return periods.

This approach aims to provide a comprehensive understanding of how urban expansion will affect watershed hydrology in the future.

## 2. Materials and Methods

### 2.1. Study Area

Charlotte is the eighth fastest-growing city in the United States, and the surrounding region is experiencing rapid urbanization [60]. According to research by the Charlotte Regional Business Alliance, this area is projected to undergo a 50% population increase by 2050, surging from 3 million to 4.5 million people [61]. Charlotte’s cost of living is 9% lower than the national average. Furthermore, the city offers affordable housing rates, approximately 23% below the national average, which is one of its most appealing features and promotes urban growth [62]. Given the swift urbanization and the looming challenges posed by climate change, it becomes imperative to comprehend the evolving hydrological dynamics of the region. Consequently, this study focuses on a watershed north of Charlotte, bordering three burgeoning cities: Mooresville, Kannapolis, and Salisbury. Each of these cities has undergone substantial growth over the past two decades. The population of Mooresville rose from 18,800 to 50,500 between 2000 and 2020, while Kannapolis witnessed an increase from 37,391 to 53,431, and Salisbury’s population grew from 26,500 to 35,600 during the same period. Based on the population growth and the watershed’s proximity to these expanding urban centers, there is an expectation that the land use patterns within the watershed will undergo substantial changes. As these cities extend outward towards the watershed, it is expected that these modifications will impact the hydrological response of the watershed. The watershed is currently predominantly characterized by agriculture and forested areas; however, it is anticipated to transform into a highly urbanized watershed in the future.

Figure 1a,b illustrate the study area’s geographical location; Figure 1c depicts the Charlotte city boundary, which was used for the prediction of LULC; and Figure 1d shows the study area watershed with prevailing CN used for assessing hydrological changes. The study area’s outlet is positioned adjacent to the Coddle Creek Reservoir in Cabarrus County, North Carolina, at geographic coordinates of approximately 35°30′14″ N degrees latitude and 80°44′11″ W degrees longitude. This outlet serves as a pivotal point for our hydrological analysis, encompassing a drainage area spanning 58.87 square kilometers. The specific station ID assigned to this outlet is USGS 0212419274, and it operates at a gauge datum of 199.73 m.

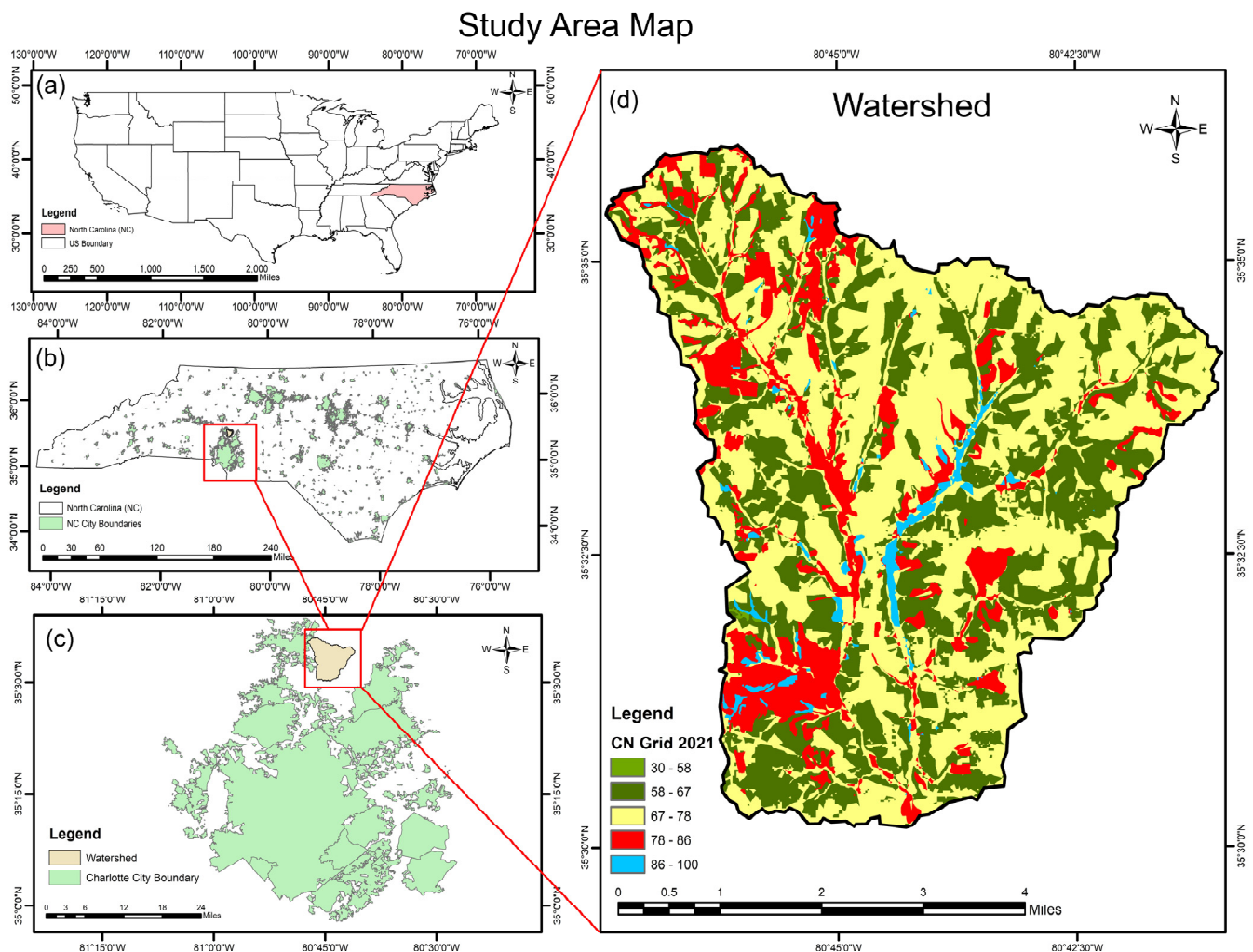


**Figure 1.** Geographical context of the study area with classification of watershed based on prevailing CN.

## 2.2. Methods

### 2.2.1. CA–Markov Model

The CA–Markov model, a widely used tool in LULC modeling, uniquely combines the Markov chain and CA concepts into a hybrid model. The Markov chain model operates as a stochastic process, assessing the likelihood of moving between states. It forecasts a system's state at a given time ( $t$ ) by relying solely on its state at a preceding time ( $t - 1$ ). Notably, this model does not consider the neighboring states of the observed cell, functioning independently in its analysis. Only using the Markov model overlooks spatial distribution, hampering its ability to predict direction accurately. Hence, the CA model becomes essential for integrating land use's spatial characteristics. In this way, the hybrid model has the ability to capture alterations in both the spatial and temporal components of land use [63]. The CA–Markov chain is an inclusive model utilized for LULC forecasting, which is integrated into the TerrSet2020 software. The formula for representing the Markov model is given in Equations (1) and (2), whereas that for CA is given in Equation (3).

$$L_t = P \times L_{t-1} \quad (1)$$

$$P = [p_{ij}] = \begin{bmatrix} p_{11} & p_{12} & \dots & p_{1m} \\ p_{21} & p_{22} & \dots & p_{2m} \\ \dots & \dots & \dots & \dots \\ p_{m1} & p_{m2} & \dots & p_{mm} \end{bmatrix} \quad (2)$$

$(0 \leq p_{ij} < 1 \text{ and } \sum_{j=1}^m p_{ij} = 1), (i, j = 1, 2, \dots, m)$

where  $P$  is the matrix of Markov transitions;  $p_{ij}$  is the element of matrix  $P$  which defines the probability of going from land use type  $i$  to  $j$ ; ( $i$  and  $j$ ) are the categories of LULC for  $t - 1$  and  $t$  time frames, respectively;  $t - 1$  and  $t$  represent two different time frames used in the model;  $m$  is the number of LULC classes; and  $L_t$  and  $L_{t-1}$  are the land use status at time  $t$  and  $t - 1$ , respectively.  $L_t$  and  $L_{t-1}$  are vectors representing fractions of different land use type at time  $t$  and  $t - 1$ , respectively.

$$L_{(t-1,t)} = f(L_{t-1}, N) \quad (3)$$

where  $L$  represents a collection of distinct and finite cellular states,  $N$  denotes the neighborhood of the cell, and  $f$  is the guideline governing the transformation of cellular states within a localized space. The use of Equations (1) and (2) can be found in [64–66], while Equation (3) can be seen in [67,68].

This study used land use data from 2001, 2013, and 2021 from the Multi-Resolution Land Characteristics (MRLC) National Land Cover Database (NLCD) map viewer. To prepare the land use data for further analysis, a series of data preprocessing steps were carried out using ArcMap, ERDAS, and QGIS. The main objective of this data preparation process was to create a consistent and compatible LULC dataset that could be seamlessly integrated into TerrSet to predict LULC changes in the years 2050 and 2080.

LULC maps were classified into five classes: water, urban area, forest, barren land, and agriculture. The driver variables that were considered to affect urban growth were topography, road networks, slope, and distance from the city center. The selection of driver variables was based on [69,70]. Markov chain analysis and CA models were used to complete the prediction in TerrSet2020, which is developed by Clark Labs [71]. The Land Change Model (LCM) in TerrSet relies on historical land cover data, transition potential maps, and Markov matrices to simulate future land cover changes. The LCM comprises three primary steps: change analysis, transition potential modeling, and change prediction. More details on the three steps can be found in [72]. This research utilizes LULC maps from 2001 and 2013 to forecast LULC conditions for 2021, subsequently validating the predictions against the actual LULC map for 2021. After the validation, maps for 2050 and 2080 were simulated from the available 2013 and 2021 LULC maps. Altuwaijri et al. [58] and Rahnama et al. [73] have used a similar approach for predicting LULC change in the future. The prediction of urbanization was carried out considering the variables for the whole of the city of Charlotte, and then the desired watershed was clipped for studying hydrological changes.

### 2.2.2. Hydrological Model Using PCSWMM

The Storm Water Management Model (SWMM) is a dynamic simulation model designed to replicate both the quantity and quality of water in urban and rural environments, covering individual events and extended-term scenarios [74]. A specialized type of stormwater modeling software, PCSWMM v7.5.3406, integrates GIS with the computational engine of the SWMM. SWMM employs non-linear reservoir theory to compute surface runoff and incorporates hydrologic abstractions, including factors like surface depression, accumulation, and infiltration on permeable surfaces. The Water Delineation Tool (WDT) within PCSWMM was employed to generate layers for flow slope, flow direction, and contributing area for individual sub-catchments based on the specified size criteria for each target sub-catchment. Subsequently, these generated layers were used to create the streams and flow path layers, which are essential for constructing the Conduits layer within the

PCSWMM system. The Conduits layer depicts the water delivery lines connecting system nodes, and the Transect object defines its non-uniform cross-section. The Transect Creator and Transect Editor tools were used to construct transects based on topography data given as the DEM layer. Input features such as Manning’s roughness, entry and exit node inverts, and length are also considered by the Conduits layer.

Various geospatial datasets were integrated to assess watershed dynamics in this hydrological analysis. These datasets included a Digital Elevation Model (DEM), Soil Data, Impervious Data, and LULC data. To facilitate this analysis, essential geometric information for the watershed, such as central lines, cross-sections, bank lines, and Manning’s n values, were generated within the HEC-RAS 6.3.1 software. These geometric data were subsequently imported into PCSWMM. The whole study area was divided into 70 sub-catchments with the help of WDT based on the 413 junctions from geometric information. The selection of PCSWMM for this specific watershed was based on the fact that the watershed’s size falls below 100 km<sup>2</sup>, and PCSWMM yields desirable simulation outcomes for catchments of this size [75]. In addition to the geometric data, CN grids were produced by overlaying hydrologic soil groups with the LULC data in ArcMap for 2021, 2050, and 2080. Subsequently, the CN for each sub-catchment was computed using the area weighted average method, a function available in PCSWMM. This step allowed for the incorporation of temporal changes in land use and land cover into the hydrological analysis. Figure 2 below illustrates the procedures conducted in the study through a methodology flowchart and Table 1 provides the sources of data downloads.

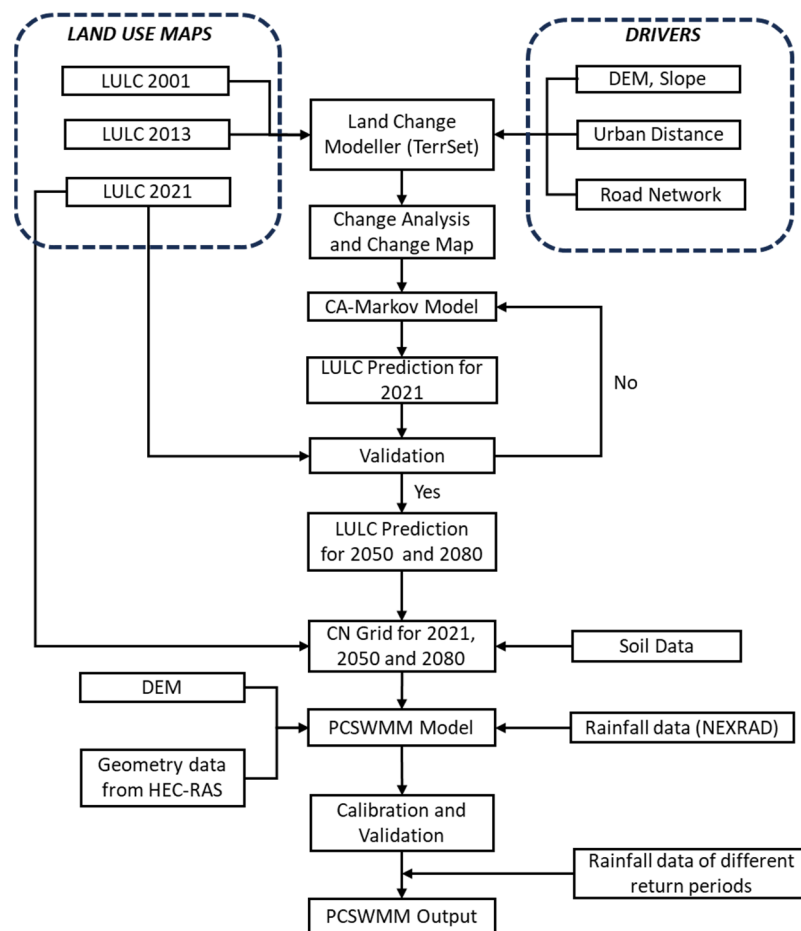


Figure 2. Methodology flowchart for LULC prediction and hydrologic modeling.

**Table 1.** Data and their sources.

| Data          | Source   |
|---------------|--|
| DEM (3 m)     | National Map viewer  |
| LULC          | Multi-Resolution Land Characteristics Consortium (MRLC)                      |
| Soil          | Geospatial Data Gateway  |
| Precipitation | National Centers for Environmental Information (NCEI), NEXRAD III Radar Data |
| Road          | Open Street Maps   |

### 2.2.3. Hydrological Model Evaluation

For proper assessment of changes in hydrologic response of the watershed due to LULC change, it is necessary to calibrate and validate the PCSWMM model. Calibration of model is made by changing the parameters to best match the observed data and then validation is done to access the calibrated parameter. This process ensures that the hydrological model is ready for further analysis. Accuracy of model was verified based on statistical metrics such as coefficient of determination ( $R^2$ ), Nash-Sutcliffe efficiency (NSE) and Percent Bias (PBIAS). The formula for above statistical parameters are listed below:

$$R^2 = \frac{\sum_{j=1}^N [(q_{j,o} - \bar{q}_o) * (q_{j,s} - \bar{q}_s)]^2}{\sum_{j=1}^N (q_{j,o} - \bar{q}_o)^2 * \sum_{j=1}^N (q_{j,s} - \bar{q}_s)^2} \quad (4)$$

$$NSE = 1 - \frac{\sum_{j=1}^N (q_{j,s} - q_{j,o})^2}{\sum_{j=1}^N (q_{j,o} - \bar{q}_o)^2} \quad (5)$$

$$PBIAS = \frac{\sum_{j=1}^N (q_{j,o} - q_{j,s})}{\sum_{j=1}^N (q_{j,o})} * 100 \quad (6)$$

where  $q_{j,o}$  is the observed flow,  $q_{j,s}$  is the simulated flow at time  $t = j$ ,  $\bar{q}_o$  and  $\bar{q}_s$  are the average observed and average simulated values, respectively and N is the total number of observations.

R-squared ( $R^2$ ) quantifies the extent to which a model accounts for variation in measured data, with a scale from 0 to 1. Larger  $R^2$  values signal reduced error variance, and those exceeding 0.5 are typically seen as satisfactory [76]. Similarly, the Nash-Sutcliffe Efficiency (NSE) spans from negative infinity to 1, where 1 signifies a flawless alignment between observed and modeled data, and values surpassing 0.5 are commonly seen as satisfactory. Moreover, Percent Bias (PBIAS) gives an idea about the average deviation of the modeled data from the observed data with 0% meaning no deviation. A model is said to be calibrated if  $PBIAS \leq \pm 10\%$  [77]. More details on the use of above equations can be found in [78].

## 3. Results

### 3.1. CA-Markov Model: Validation

This study employed area under the curve (AUC) of Total Operating Characteristic (TOC) and a cross-tabulation method comparing three maps to validate the model. This method assesses both the elements of agreement and disagreement between the maps. The TOC method assesses the model's effectiveness in predicting change, whereas the cross-tabulation matrix involving the three maps offers in-depth insights into the accuracy of predicted changes and the persistence of each land cover class. The three maps used here are the study reference map (LULC of 2013), original map (LULC 2021), and predicted map (LULC 2021 simulated). [79,80] propose two agreement components—Hits and Correct Rejection—and three disagreement components—Misses, False Alarm, and Wrong Hits. These metrics serve as an alternative to Kappa statistics. Kappa indices compare accuracy

to randomness, which is not suitable for map construction and can falsely indicate high accuracy. Thus, Pontius and Millones [80] metrics offer a more reasonable approach, focusing on agreement and disagreement components which are given in Table 2. The model had an AUC of 0.84, which deems the prediction is satisfactory for further analysis.

**Table 2.** Percentage of validation parameters obtained after comparing predicted and actual image of 2021.

| Agreement Components | %     | Disagreement Components | %     |
|----------------------|-------|-------------------------|-------|
| Hits                 | 3.10  | Wrong Hits              | 4.70  |
| Correct Rejection    | 68    | False Alarms            | 9.30  |
|                      |       | Misses                  | 14.90 |
| Total                | 71.10 | Total                   | 28.90 |

### 3.2. PCSWMM: Calibration and Validation

Calibration and validation of model was done for an event-scale rainfall. Due to the unavailability of reliable gauged precipitation data for the watershed, this study considered the use of NEXRAD precipitation data from the RAS Mapper of PCSWMM for calibration and validation of the model. NEXRAD precipitation has a spatial resolution of 4 km and has very high accuracy when compared to other satellite-based precipitation data [81]. Bhusal et al. [82] and Hamed et al. [83] have demonstrated the effectiveness of NEXRAD precipitation data in regions lacking reliable gauge precipitation data, producing satisfactory results. It's important to note that while gauge precipitation data fails to capture the spatial variability of precipitation, radar precipitation data excels in this regard. The RAS Mapper creates a precipitation dataset for each of the sub-catchments, which is then applied to the model.

Factors such as manning's n and the area of the sub-catchments were adjusted so that the observed value at the outlet matches the simulated value from the model for the calibration and validation of the model. A single hydrologic event on 11 November 2020–14 November 2020 was used for calibration, and an event on 5 February 2020–8 February 2020 was used to validate the hydrologic model, shown in Figure 3. The statistical parameters such as  $R^2$ , NSE, and PBIAS were calculated for two events and are shown in the Table 3.

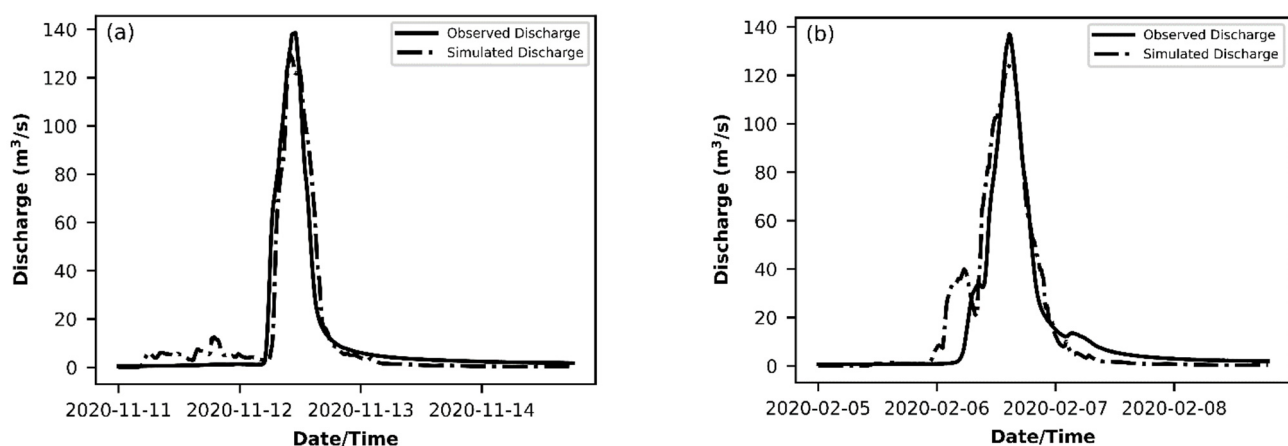


**Figure 3.** Graphical representation of observed and simulated discharge during (a) calibration and (b) validation.

**Table 3.** Statistical evaluation of observed and simulated discharge hydrograph for the watershed.

| Events | Date             | Parameter      |      |       |
|--------|------------------|----------------|------|-------|
|        |                  | R <sup>2</sup> | NSE  | PBIAS |
| 1      | 11 November 2020 | 0.91           | 0.87 | 1.45% |
| 2      | 5 February 2020  | 0.88           | 0.83 | 8.70% |

3.3. LULC Change

To assess the alterations in hydrological response in the future, it was essential to forecast the LULC change for 2050 and 2080. The spatial distribution of LULC changes for 2021, 2050, and 2080 is illustrated in Figure 4 and quantified in Table 4.

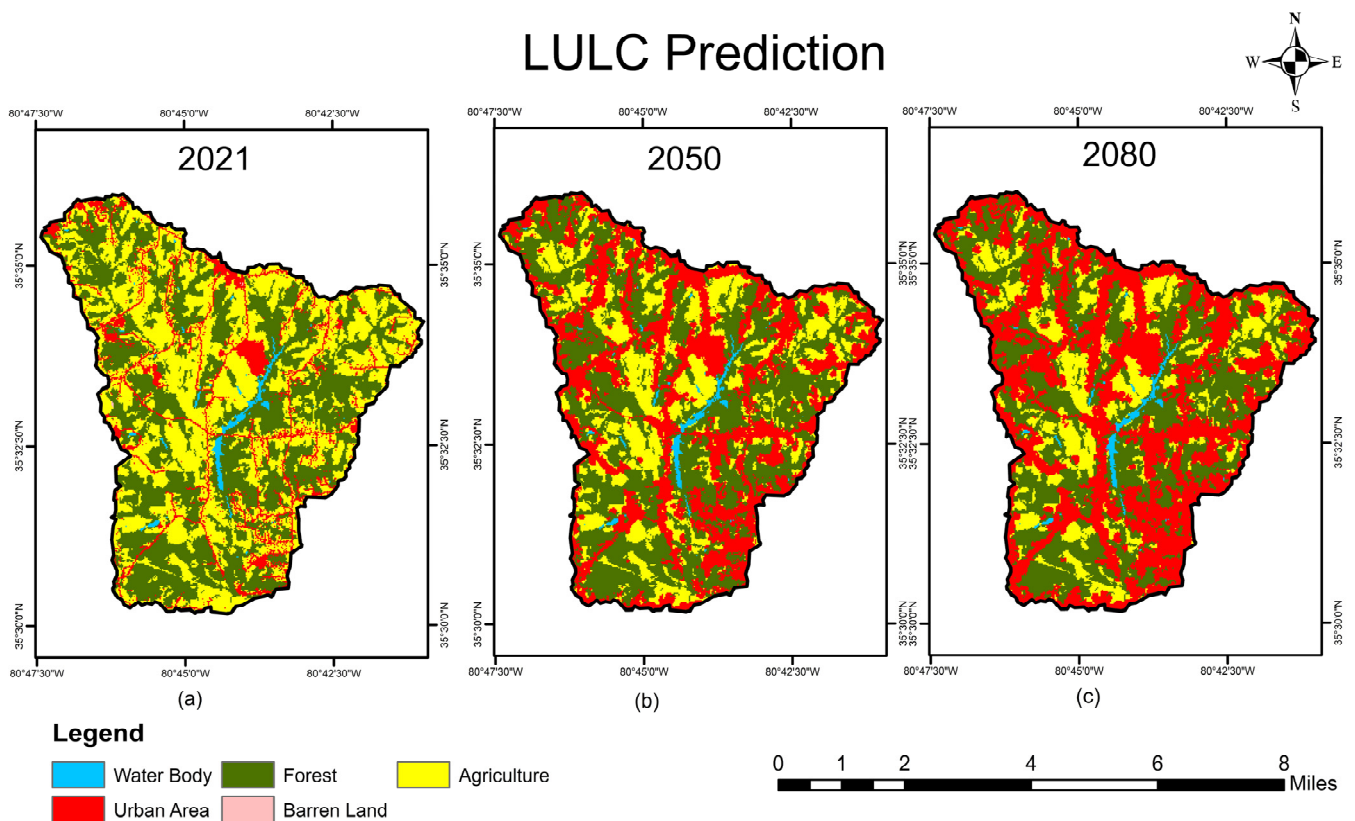


**Figure 4.** Predicted LULC for (a) 2021, (b) 2050, and (c) 2080 using CA-Markov model.

**Table 4.** LULC change with percentage of area covered for observed and simulated.

| LULC/Year   | Observed        |      |                 |      |                 |      | Simulated       |      |                 |      |                 |      |
|-------------|-----------------|------|-----------------|------|-----------------|------|-----------------|------|-----------------|------|-----------------|------|
|             | 2001            |      | 2013            |      | 2021            |      | 2021            |      | 2050            |      | 2080            |      |
|             | km <sup>2</sup> | %    |
| Water Body  | 0.70            | 1.2  | 0.69            | 1.2  | 0.69            | 1.2  | 0.67            | 1.1  | 0.67            | 1.1  | 0.67            | 1.1  |
| Urban Area  | 5.96            | 10.1 | 7.11            | 12.1 | 6.82            | 11.6 | 7.13            | 12.1 | 20.09           | 34.1 | 26.0            | 44.2 |
| Forest      | 26.39           | 44.8 | 25.25           | 42.9 | 25.50           | 43.3 | 25.39           | 43.2 | 25.17           | 42.8 | 22.2            | 37.7 |
| Barren      | 0.01            | 0.0  | 0.01            | 0.0  | 0.01            | 0.0  | 0.01            | 0.0  | 0.00            | 0.0  | 0.00            | 0.0  |
| Agriculture | 25.81           | 43.9 | 25.81           | 43.8 | 25.85           | 43.9 | 25.67           | 43.6 | 12.94           | 22.0 | 9.99            | 22.0 |

Notably, the map from Figure 4 indicates a substantial decrease in the green and yellow areas and a significant expansion of built-up areas in the watershed. As the study area sits between three expanding cities, it's noticeable that the LULC has retained a relatively steady pattern from 2001 to 2021, aligning with the growth experienced by these

cities during this time frame. However, once the cities' urbanization peaked, the built-up areas started to encroach towards the watershed. As a result, a rise in the built-up areas can be seen for the year 2050 and 2080.

The study area shows an increase of urban areas by approximately 13 km<sup>2</sup> and 20 km<sup>2</sup> from the original 7 km<sup>2</sup> for the years 2050 and 2080, respectively, compared to the urban area in 2021. Most of the increase has been accompanied by the loss of agricultural area, whereas a small portion has been contributed from forest and barren land. This is because of road networks being developed around the vicinity of agricultural areas. In 2021, the watershed's built-up area made up only 12% of its entire size, with forests and farmland making up the majority of the land cover. However, by 2050 and 2080, this figure rose substantially to 34% and 44% of the total watershed area, signifying a notable rise in the built-up area. The expansion of urbanization will lead to an elevation in the curve number of sub-catchments, mainly due to the increased presence of impervious surfaces within the watershed.

### 3.4. Effect of LULC Change on Streamflow

The findings of the LULC prediction show that the watershed underwent a significant amount of land use change. The LULC patterns predicted from TerrSET were then processed in ArcMap to create CN grids for both 2050 and 2080, which were then used as the direct inputs in the validated PCSWMM model to generate CN values for the delineated 70 sub-catchments. Runoff in PCSWMM can be calculated with the CN method for infiltration, which is computationally efficient and a popular method for estimating runoff [84,85].

This research investigates how future LULC changes affect peak discharge and runoff volume in storms with return intervals of 10, 50, and 100 years (Table 5). Peak discharge exhibited a 5% and 6.8% rise in the 2050 and 2080 LULC scenarios for a storm event of 100-year magnitude. For a 50-year storm event, the increase amounted to 14.4% and 18.2%; during a 10-year storm event, it surged to 17.1% and 30.1%. The escalation in peak discharge was significant for smaller storm events and reduced as the storm event size increased. Runoff volume continued to rise as the size of the storm event continued to increase. Similarly, as in the case of peak discharge, the rise in runoff volume was much more significant for smaller events as compared to larger storm events.

**Table 5.** Comparison of peak discharge and runoff volumes for 2021, 2050, and 2080 with different return periods.

| Return Period | Year | Peak Discharge (m <sup>3</sup> /s) | Runoff Volume (m <sup>3</sup> ) | Percentage Change Compared to 2021 |               |
|---------------|------|------------------------------------|---------------------------------|------------------------------------|---------------|
|               |      |                                    |                                 | Peak Discharge                     | Runoff Volume |
| T = 10 yrs    | 2021 | 288.23                             | 4,361,300                       |                                    |               |
|               | 2050 | 337.52                             | 4,691,500                       | 17.1%                              | 7.6%          |
|               | 2080 | 374.99                             | 5,186,000                       | 30.1%                              | 18.9%         |
| T = 50 yrs    | 2021 | 450.73                             | 6,197,700                       |                                    |               |
|               | 2050 | 515.74                             | 6,778,600                       | 14.4%                              | 9.4%          |
|               | 2080 | 532.65                             | 7,149,800                       | 18.2%                              | 15.4%         |
| T = 100 yrs   | 2021 | 512.72                             | 6,891,900                       |                                    |               |
|               | 2050 | 538.58                             | 7,441,700                       | 5.0%                               | 8.0%          |
|               | 2080 | 547.62                             | 7,810,100                       | 6.8%                               | 13.3%         |

Urban land had the highest CN values among the five land use types that this study investigated, followed by barren land, agricultural, and forest areas. The relationship outlined by [86] indicates that land use types with lower CN values possess greater infiltration capacities. Because of their decreased capacity to absorb or intercept rainfall, surfaces with greater CN values are thus considered more vulnerable to flooding. Since surface impermeability increases due to urbanization, the runoff production from the basin has increased and flood peaks and volumes have increased.

#### 4. Discussion and Conclusions

This research utilized a combined method involving a land use transition model (CA–Markov) and an event-specific hydrological model (PCSWMM) to assess how future changes in land use might affect storm runoff generation within a rapidly urbanizing watershed, specifically considering simulated rainstorm scenarios. The findings can be summarized as follows: Firstly, a significant shift in land use was noted, transitioning from agricultural and forest areas to urban development. This transformation makes it an ideal case study area for assessing alterations in hydrological responses. Secondly, as urbanization progresses within the watershed, the projected land use changes predicted by CA–Markov indicate an increase in runoff volume and peak discharge levels relative to the 2021 land use patterns. Thirdly, the effects of changes in land use are notably significant during periods of moderately frequent and less intense rainfall, yet they exhibit minimal impact during extreme rainfall events.

The declining sensitivity of hydrology to land use alterations during high-frequency events aligns with the observations made by Chen et al. [87] and Gao et al. [88]. The most significant land use change witnessed during the study period involved a 20 km<sup>2</sup> increase in urbanization, predominantly at the expense of agricultural and forested areas. According to predictions based on land use and other similar studies like [89,90], this shift is expected to heighten peak runoff within the watershed. This increase stems from the reduction in the watershed's innate capacity to absorb rainfall, leading to varied increments in flood quantities. Moreover, the research highlights that smaller floods are especially affected by the decrease in surface permeability, underscoring the significant impact of urbanization on hydrological responses.

The methodology employed in this study showcased how utilizing predicted land use data from a land change modeler can effectively assess the impact on a watershed through an event-specific hydrological model like PCSWMM. The methodology, complemented by quantitative outcomes such as hydrographs and tabulated data, provides a valuable resource for authorities. It enables the scientific formulation of land use policies and the implementation of appropriate stormwater infrastructure measures. Moreover, it is crucial to establish policy measures aimed at encouraging the widespread adoption of Low-Impact Development (LID) techniques. These measures are supported by numerous research studies that have consistently shown their effectiveness in mitigating the rise in peak runoff resulting from urbanization [91–93]. The primary goal is to reduce peak runoff and alleviate the risks associated with flooding. As a result, this method holds promise as a supportive tool for decision-making in watershed land use planning and management.

The current study's LULC mapping methodology, based on four primary drivers, could be significantly refined for better accuracy by including additional variables such as population density, socio-economic aspects, policy factors, and proximity to key facilities like hospitals and schools. These factors directly influence changes in land use patterns. By integrating them, the model would provide a more holistic and accurate view of potential shifts. Future research endeavors should aim to incorporate these variables into LULC models and also add machine learning approaches to CA–Markov for a more precise representation of land use change [94,95]. Moreover, there is no inclusion of the potential effect of climate change on the hydrological response in the watershed, which is a notable limitation of this study. Incorporating the effects of climate change on stormwater runoff, alongside LULC alterations, would provide a comprehensive perspective on the hydrological dynamics of the watershed. This approach would enhance the effectiveness of the model for planning and decision-making. Future research should prioritize integrating the effects of climate change to improve the accuracy and applicability of hydrological predictions.

**Author Contributions:** Conceptualization, A.K.; methodology, A.B.; software, M.B. and A.B.G.; formal analysis, M.B. and A.B.G.; writing—original draft preparation, M.B., A.B.G. and A.B.; writing—review and editing, M.B., A.B.G., A.B. and A.K.; supervision, A.K. All authors have read and agreed to the published version of the manuscript.

**Funding:** This research received no external funding.

**Data Availability Statement:** The data used in the study are freely available online and has been mentioned in the method section.

**Acknowledgments:** The authors thank the editor and two anonymous reviewers for their insights to enhance the clarity of the manuscript. The authors would like to acknowledge Computational Hydraulics International for providing free academic access to PCSWMM for research.

**Conflicts of Interest:** Author Amrit Bhusal was employed by the company Arcadis U.S., Inc. The remaining authors declare that the research was conducted in the absence of any commercial or financial relationships that could be construed as a potential conflict of interest.

## References

1. Liu, Y.; Huang, X.; Yang, H.; Zhong, T. Environmental effects of land-use/cover change caused by urbanization and policies in Southwest China Karst area—A case study of Guiyang. *Habitat Int.* **2014**, *44*, 339–348. [[CrossRef](#)]
2. Torbick, N.M.; Qi, J.; Roloff, G.J.; Stevenson, R.J. Investigating Impacts of Land-Use Land Cover Change on Wetlands in the Muskegon River Watershed, Michigan, USA. *Wetlands* **2006**, *26*, 1103–1113. [[CrossRef](#)]
3. Hassan, M.M.; Nazem, M.N.I. Examination of Land Use/Land Cover Changes, Urban Growth Dynamics, and Environmental Sustainability in Chittagong City, Bangladesh. *Environ. Dev. Sustain.* **2016**, *18*, 697–716. [[CrossRef](#)]
4. Van Vliet, J.; de Groot, H.L.; Rietveld, P.; Verburg, P.H. Manifestations and Underlying Drivers of Agricultural Land Use Change in Europe. *Landsc. Urban Plan.* **2015**, *133*, 24–36. [[CrossRef](#)]
5. Lant, C.; Stoebner, T.J.; Schoof, J.T.; Crabb, B. The Effect of Climate Change on Rural Land Cover Patterns in the Central United States. *Clim. Chang.* **2016**, *138*, 585–602. [[CrossRef](#)]
6. Birhanu, A.; Masih, I.; Van Der Zaag, P.; Nyssen, J.; Cai, X. Impacts of Land Use and Land Cover Changes on Hydrology of the Gumara Catchment, Ethiopia. *Phys. Chem. Earth Parts A/B/C* **2019**, *112*, 165–174. [[CrossRef](#)]
7. Yin, J.; He, F.; Xiong, Y.J.; Qiu, G.Y. Effects of Land Use/Land Cover and Climate Changes on Surface Runoff in a Semi-Humid and Semi-Arid Transition Zone in Northwest China. *Hydrol. Earth Syst. Sci.* **2017**, *21*, 183–196. [[CrossRef](#)]
8. Aryal, A.; Acharya, A.; Kalra, A. Assessing the Implication of Climate Change to Forecast Future Flood Using CMIP6 Climate Projections and HEC-RAS Modeling. *Forecasting* **2022**, *4*, 582–603. [[CrossRef](#)]
9. Pradhan-Salike, I.; Pokharel, J.R. Impact of Urbanization and Climate Change on Urban Flooding: A Case of the Kathmandu Valley. *JNRD J. Nat. Resour. Dev.* **2017**, *7*, 56–66. [[CrossRef](#)]
10. Pumo, D.; Arnone, E.; Francipane, A.; Caracciolo, D.; Noto, L.V. Potential Implications of Climate Change and Urbanization on Watershed Hydrology. *J. Hydrol.* **2017**, *554*, 80–99. [[CrossRef](#)]
11. Sadeghi, S.M.M.; Gordon, D.A.; Van Stan, J.T., II. A Global Synthesis of Throughfall and Stemflow Hydrometeorology. In *Precipitation Partitioning by Vegetation: A Global Synthesis*; Van Stan, I., John, T., Gutmann, E., Friesen, J., Eds.; Springer International Publishing: Cham, Switzerland, 2020; pp. 49–70. ISBN 978-3-030-29702-2. [[CrossRef](#)]
12. Wang, Y.; Li, C.; Liu, M.; Cui, Q.; Wang, H.; Lv, J.; Li, B.; Xiong, Z.; Hu, Y. Spatial Characteristics and Driving Factors of Urban Flooding in Chinese Megacities. *J. Hydrol.* **2022**, *613*, 128464. [[CrossRef](#)]
13. Vörösmarty, C.J.; Green, P.; Salisbury, J.; Lammers, R.B. Global Water Resources: Vulnerability from Climate Change and Population Growth. *Science* **2000**, *289*, 284–288. [[CrossRef](#)]
14. Okello, C.; Tomasello, B.; Greggio, N.; Wambiji, N.; Antonellini, M. Impact of Population Growth and Climate Change on the Freshwater Resources of Lamu Island, Kenya. *Water* **2015**, *7*, 1264–1290. [[CrossRef](#)]
15. Aluko, O.E. The Impact of Urbanization on Housing Development: The Lagos Experience, Nigeria. *Ethiop. J. Environ. Stud. Manag.* **2010**, *3*. [[CrossRef](#)]
16. Suriya, S.; Mudgal, B.V. Impact of Urbanization on Flooding: The Thirusoolam Sub Watershed—A Case Study. *J. Hydrol.* **2012**, *412–413*, 210–219. [[CrossRef](#)]
17. Feng, B.; Zhang, Y.; Bourke, R. Urbanization impacts on flood risks based on urban growth data and coupled flood models. *Nat. Hazards* **2021**, *106*, 613–627. [[CrossRef](#)]
18. White, M.D.; Greer, K.A. The Effects of Watershed Urbanization on the Stream Hydrology and Riparian Vegetation of Los Penasquitos Creek, California. *Landsc. Urban Plan.* **2006**, *74*, 125–138. [[CrossRef](#)]
19. Woldesenbet, T.A.; Elagib, N.A.; Ribbe, L.; Heinrich, J. Catchment response to climate and land use changes in the Upper Blue Nile sub-basins, Ethiopia. *Sci. Total Environ.* **2018**, *644*, 193–206. [[CrossRef](#)]
20. Dwarakish, G.S.; Ganasri, B.P. Impact of Land Use Change on Hydrological Systems: A Review of Current Modeling Approaches. *Cogent Geosci.* **2015**, *1*, 1115691. [[CrossRef](#)]
21. Gashaw, T.; Tulu, T.; Argaw, M.; Worqlul, A.W. Modeling the Hydrological Impacts of Land Use/Land Cover Changes in the Andassa Watershed, Blue Nile Basin, Ethiopia. *Sci. Total Environ.* **2018**, *619–620*, 1394–1408. [[CrossRef](#)]
22. Masih, I.; Maskey, S.; Uhlenbrook, S.; Smakhtin, V. Impact of Upstream Changes in Rain-Fed Agriculture on Downstream Flow in a Semi-Arid Basin. *Agric. Water Manag.* **2011**, *100*, 36–45. [[CrossRef](#)]

23. Nie, W.; Yuan, Y.; Kepner, W.; Nash, M.S.; Jackson, M.; Erickson, C. Assessing Impacts of Landuse and Landcover Changes on Hydrology for the Upper San Pedro Watershed. *J. Hydrol.* **2011**, *407*, 105–114. [[CrossRef](#)]
24. Getachew, H.E.; Melesse, A.M. The Impact of Land Use Change on the Hydrology of the Angereb Watershed, Ethiopia. *Int. J. Water Sci.* **2012**, *1*. [[CrossRef](#)]
25. Welde, K.; Gebremariam, B. Effect of Land Use Land Cover Dynamics on Hydrological Response of Watershed: Case Study of Tekeze Dam Watershed, Northern Ethiopia. *Int. Soil Water Conserv. Res.* **2017**, *5*, 1–16. [[CrossRef](#)]
26. Brody, S.; Blessing, R.; Sebastian, A.; Bedient, P. Examining the Impact of Land Use/Land Cover Characteristics on Flood Losses. *J. Environ. Plan. Manag.* **2014**, *57*, 1252–1265. [[CrossRef](#)]
27. Gao, J.; Holden, J.; Kirkby, M. The Impact of Land-cover Change on Flood Peaks in Peatland Basins. *Water Resour. Res.* **2016**, *52*, 3477–3492. [[CrossRef](#)]
28. Setegn, S.G.; Srinivasan, R.; Dargahi, B. Hydrological Modelling in the Lake Tana Basin, Ethiopia Using SWAT Model. *Open Hydrol. J.* **2008**, *2*, 49–62. [[CrossRef](#)]
29. Gebremicael, T.G.; Mohamed, Y.A.; Betrie, G.D.; van der Zaag, P.; Teferi, E. Trend Analysis of Runoff and Sediment Fluxes in the Upper Blue Nile Basin: A Combined Analysis of Statistical Tests, Physically-Based Models and Landuse Maps. *J. Hydrol.* **2013**, *482*, 57–68. [[CrossRef](#)]
30. Neupane, R.P.; Kumar, S. Estimating the Effects of Potential Climate and Land Use Changes on Hydrologic Processes of a Large Agriculture Dominated Watershed. *J. Hydrol.* **2015**, *529*, 418–429. [[CrossRef](#)]
31. Huong, H.T.L.; Pathirana, A. Urbanization and Climate Change Impacts on Future Urban Flooding in Can Tho City, Vietnam. *Hydrol. Earth Syst. Sci.* **2013**, *17*, 379–394. [[CrossRef](#)]
32. Shanableh, A.; Al-Ruzouq, R.; Yilmaz, A.G.; Siddique, M.; Merabtene, T.; Imteaz, M.A. Effects of Land Cover Change on Urban Floods and Rainwater Harvesting: A Case Study in Sharjah, UAE. *Water* **2018**, *10*, 631. [[CrossRef](#)]
33. Bahremand, A.; De Smedt, F.; Corluy, J.; Liu, Y.B.; Poorova, J.; Velcicka, L.; Kunikova, E. WetSpa Model Application for Assessing Reforestation Impacts on Floods in Margecany–Hornad Watershed, Slovakia. *Water Resour. Manag.* **2007**, *21*, 1373–1391. [[CrossRef](#)]
34. Somvanshi, S.S.; Bhalla, O.; Kunwar, P.; Singh, M.; Singh, P. Monitoring Spatial LULC Changes and Its Growth Prediction Based on Statistical Models and Earth Observation Datasets of Gautam Budh Nagar, Uttar Pradesh, India. *Environ. Dev. Sustain.* **2020**, *22*, 1073–1091. [[CrossRef](#)]
35. Das, S.; Sarkar, R. Predicting the Land Use and Land Cover Change Using Markov Model: A Catchment Level Analysis of the Bhagirathi-Hugli River. *Spat. Inf. Res.* **2019**, *27*, 439–452. [[CrossRef](#)]
36. Mozaffaree Pour, N.; Oja, T. Prediction Power of Logistic Regression (LR) and Multi-Layer Perceptron (MLP) Models in Exploring Driving Forces of Urban Expansion to Be Sustainable in Estonia. *Sustainability* **2021**, *14*, 160. [[CrossRef](#)]
37. Feng, C.; Zhang, N.; Habiyaqare, T.; Yu, H. Development of a Cellular Automata-Based Distributed Hydrological Model for Simulating Urban Surface Runoff. *J. Hydrol.* **2023**, *627*, 130348. [[CrossRef](#)]
38. Rahman, M.T.U.; Tabassum, F.; Rasheduzzaman, M.; Saba, H.; Sarkar, L.; Ferdous, J.; Uddin, S.Z.; Zahedul Islam, A.Z.M. Temporal Dynamics of Land Use/Land Cover Change and Its Prediction Using CA-ANN Model for Southwestern Coastal Bangladesh. *Environ. Monit. Assess.* **2017**, *189*, 565. [[CrossRef](#)]
39. Tong, X.; Feng, Y. A Review of Assessment Methods for Cellular Automata Models of Land-Use Change and Urban Growth. *Int. J. Geogr. Inf. Sci.* **2020**, *34*, 866–898. [[CrossRef](#)]
40. Tan, X.; Deng, M.; Chen, K.; Shi, Y.; Zhao, B.; Liu, Q. A Spatial Hierarchical Learning Module Based Cellular Automata Model for Simulating Urban Expansion: Case Studies of Three Chinese Urban Areas. *GIScience Remote Sens.* **2024**, *61*, 2290352. [[CrossRef](#)]
41. Clarke, K.C.; Hoppen, S.; Gaydos, L. A Self-Modifying Cellular Automaton Model of Historical Urbanization in the San Francisco Bay Area. *Environ. Plann. B* **1997**, *24*, 247–261. [[CrossRef](#)]
42. Sang, L.; Zhang, C.; Yang, J.; Zhu, D.; Yun, W. Simulation of Land Use Spatial Pattern of Towns and Villages Based on CA–Markov Model. *Math. Comput. Model.* **2011**, *54*, 938–943. [[CrossRef](#)]
43. Wagner, D.F. Cellular Automata and Geographic Information Systems. *Environ. Plann. B Plann. Des.* **1997**, *24*, 219–234. [[CrossRef](#)]
44. Aburas, M.M.; Ho, Y.M.; Ramli, M.F.; Ash'aari, Z.H. The Simulation and Prediction of Spatio-Temporal Urban Growth Trends Using Cellular Automata Models: A Review. *Int. J. Appl. Earth Obs. Geoinf.* **2016**, *52*, 380–389. [[CrossRef](#)]
45. Noszczyk, T. A Review of Approaches to Land Use Changes Modeling. *Hum. Ecol. Risk Assess. Int. J.* **2019**, *25*, 1377–1405. [[CrossRef](#)]
46. Almeida, C.M.; Gleriani, J.M.; Castejon, E.F.; Soares-Filho, B.S. Using Neural Networks and Cellular Automata for Modelling Intra-urban Land-use Dynamics. *Int. J. Geogr. Inf. Sci.* **2008**, *22*, 943–963. [[CrossRef](#)]
47. Rozos, E.; Butler, D.; Makropoulos, C. An Integrated System Dynamics–Cellular Automata Model for Distributed Water-Infrastructure Planning. *Water Sci. Technol. Water Supply* **2016**, *16*, 1519–1527. [[CrossRef](#)]
48. Mustafa, A.; Cools, M.; Saadi, I.; Teller, J. Coupling Agent-Based, Cellular Automata and Logistic Regression into a Hybrid Urban Expansion Model (HUEM). *Land Use Policy* **2017**, *69*, 529–540. [[CrossRef](#)]
49. Gaur, S.; Mittal, A.; Bandyopadhyay, A.; Holman, I.; Singh, R. Spatio-temporal analysis of land use and land cover change: A systematic model inter-comparison driven by integrated modelling techniques. *Int. J. Remote Sens.* **2020**, *41*, 9229–9255. [[CrossRef](#)]
50. Kumar, V.; Singh, V.K.; Gupta, K.; Jha, A.K. Integrating Cellular Automata and Agent-Based Modeling for Predicting Urban Growth: A Case of Dehradun City. *J. Indian Soc. Remote Sens.* **2021**, *49*, 2779–2795. [[CrossRef](#)]

51. Ghosh, P.; Mukhopadhyay, A.; Chanda, A.; Mondal, P.; Akhand, A.; Mukherjee, S.; Nayak, S.K.; Ghosh, S.; Mitra, D.; Ghosh, T. Application of Cellular Automata and Markov-Chain Model in Geospatial Environmental Modeling—A Review. *Remote Sens. Appl. Soc. Environ.* **2017**, *5*, 64–77. [CrossRef]
52. Zhang, Z.; Hu, B.; Jiang, W.; Qiu, H. Identification and Scenario Prediction of Degree of Wetland Damage in Guangxi Based on the CA-Markov Model. *Ecol. Indic.* **2021**, *127*, 107764. [CrossRef]
53. Mondal, M.S.; Sharma, N.; Garg, P.K.; Kappas, M. Statistical Independence Test and Validation of CA Markov Land Use Land Cover (LULC) Prediction Results. *Egypt. J. Remote Sens. Space Sci.* **2016**, *19*, 259–272. [CrossRef]
54. Eastman, J.R. *IDRISI Guide to GIS and Image Processing*. Accessed in *IDRISI Selva 1*; Clark University: Worcester, MA, USA, 2009; pp. 182–185.
55. Amini Parsa, V.; Yavari, A.; Nejadi, A. Spatio-Temporal Analysis of Land Use/Land Cover Pattern Changes in Arasbaran Biosphere Reserve: Iran. *Model. Earth Syst. Environ.* **2016**, *2*, 1–13. [CrossRef]
56. Huang, Y.; Yang, B.; Wang, M.; Liu, B.; Yang, X. Analysis of the Future Land Cover Change in Beijing Using CA-Markov Chain Model. *Environ. Earth Sci.* **2020**, *79*, 60. [CrossRef]
57. Subedi, P.; Subedi, K.; Thapa, B. Application of a Hybrid Cellular Automaton-Markov (CA-Markov) Model in Land-Use Change Prediction: A Case Study of Saddle Creek Drainage Basin, Florida. *Appl. Ecol. Environ. Sci.* **2013**, *1*, 126–132. [CrossRef]
58. Altuwaijri, H.A.; Alotaibi, M.H.; Almudlaj, A.M.; Almalki, F.M. Predicting Urban Growth of Arriyadh City, Capital of the Kingdom of Saudi Arabia, Using Markov Cellular Automata in TerrSet Geospatial System. *Arab. J. Geosci.* **2019**, *12*, 135. [CrossRef]
59. Karimi, H.; Jafarnezhad, J.; Khaleidi, J.; Ahmadi, P. Monitoring and prediction of land use/land cover changes using CA-Markov model: A case study of Ravansar County in Iran. *Arab. J. Geosci.* **2018**, *11*, 1–9. [CrossRef]
60. Charlotte Is the 8th Fastest-Growing City in the US. *Praise 100.9*; 2022. Available online: <https://www.wcnc.com/article/money/charlotte-8th-fastest-growing-us-city-unc-research-shows/275-bcf59ea5-e00f-4aba-bdba-5fb6d74cdcaf> (accessed on 13 September 2023).
61. Charlotte Region Expected to Grow 50 Percent by 2050. Available online: <https://www.wcnc.com/article/news/local/charlotte-region-expected-to-grow-50-percent-by-2050-population-growth-york-lancaster-diversity-south-carolina-north-carolina/275-33158760-d79f-4c2c-9da0-eb368e4ca5bf> (accessed on 12 September 2023).
62. Why Charlotte Is One of the Fastest Growing Cities, Ever. *Henderson Properties*; 2022. Available online: <https://www.hendersonproperties.com/2022/05/charlotte-fast-growth/> (accessed on 13 September 2023).
63. Houet, T.; Hubert-Moy, L. Modeling and projecting land-use and land-cover changes with Cellular Automaton in considering landscape trajectories. *EARSeL eProc.* **2006**, *5*, 63–76. Available online: <https://shs.hal.science/halshs-00195847/document> (accessed on 19 November 2023).
64. Tang, J.; Wang, L.; Yao, Z. Spatio-temporal Urban Landscape Change Analysis Using the Markov Chain Model and a Modified Genetic Algorithm. *Int. J. Remote Sens.* **2007**, *28*, 3255–3271. [CrossRef]
65. Azizi, A.; Malakmohamadi, B.; Jafari, H.R. Land Use and Land Cover Spatiotemporal Dynamic Pattern and Predicting Changes Using Integrated CA-Markov Model. *Glob. J. Environ. Sci. Manag.* **2016**, *2*, 223–234. [CrossRef]
66. Gong, W.; Yuan, L.; Fan, W.; Stott, P. Analysis and Simulation of Land Use Spatial Pattern in Harbin Prefecture Based on Trajectories and Cellular Automata—Markov Modelling. *Int. J. Appl. Earth Obs. Geoinf.* **2015**, *34*, 207–216. [CrossRef]
67. Lu, Y.; Wu, P.; Ma, X.; Li, X. Detection and Prediction of Land Use/Land Cover Change Using Spatiotemporal Data Fusion and the Cellular Automata-Markov Model. *Environ. Monit. Assess.* **2019**, *191*, 68. [CrossRef]
68. Aliani, H.; Malmir, M.; Sourodi, M.; Kafaky, S.B. Change Detection and Prediction of Urban Land Use Changes by CA-Markov Model (Case Study: Talesh County). *Environ. Earth Sci.* **2019**, *78*, 546. [CrossRef]
69. Camara, M.; Jamil, N.R.B.; Abdullah, A.F.B.; Hashim, R.B. Integrating Cellular Automata Markov Model to Simulate Future Land Use Change of a Tropical Basin. *Glob. J. Environ. Sci. Manag.* **2020**, *6*, 403–414. [CrossRef]
70. Razaai, N.H.; Abdullah, S.A.; Reza, M.I.H. Identifying Factors and Predicting the Future Land-Use Change of Protected Area in the Agricultural Landscape of Malaysian Peninsula for Conservation Planning. *Remote Sens. Appl. Soc. Environ.* **2020**, *18*, 100298. [CrossRef]
71. Eastman, J.R. *TerrSet 2020 Geospatial Monitoring and Modeling System*; Clark Labs, Clark University: Worcester, MA, USA, 2020.
72. Azari, M.; Billa, L.; Chan, A. Multi-Temporal Analysis of Past and Future Land Cover Change in the Highly Urbanized State of Selangor, Malaysia. *Ecol. Process.* **2022**, *11*, 2. [CrossRef]
73. Rahnama, M.R. Forecasting Land-Use Changes in Mashhad Metropolitan Area Using Cellular Automata and Markov Chain Model for 2016–2030. *Sustain. Cities Soc.* **2021**, *64*, 102548. [CrossRef]
74. Gironás, J.; Roesner, L.A.; Davis, J.; Rossman, L.A.; Supply, W. *Storm Water Management Model Applications Manual*; National Risk Management Research Laboratory, Office of Research and Development, US Environmental Protection Agency: Cincinnati, OH, USA, 2009.
75. Akhter, M.S.; Hewa, G.A. The Use of PCSWMM for Assessing the Impacts of Land Use Changes on Hydrological Responses and Performance of WSUD in Managing the Impacts at Myponga Catchment, South Australia. *Water* **2016**, *8*, 511. [CrossRef]
76. Di Bucchianico, A. *Coefficient of determination (R<sup>2</sup>)*. *Encyclopedia of Statistics in Quality and Reliability*; John Wiley & Sons, Ltd.: New Jersey, NY, USA, 2008. [CrossRef]

77. Gupta, H.V.; Sorooshian, S.; Yapo, P.O. Status of automatic calibration for hydrologic models: Comparison with multilevel expert calibration. *J. Hydrol. Eng.* **1999**, *4*, 135–143. [[CrossRef](#)]
78. Althoff, D.; Rodrigues, L.N. Goodness-of-Fit Criteria for Hydrological Models: Model Calibration and Performance Assessment. *J. Hydrol.* **2021**, *600*, 126674. [[CrossRef](#)]
79. Pontius, R.G.; Peethambaram, S.; Castella, J.-C. Comparison of Three Maps at Multiple Resolutions: A Case Study of Land Change Simulation in Cho Don District, Vietnam. *Ann. Assoc. Am. Geogr.* **2011**, *101*, 45–62. [[CrossRef](#)]
80. Pontius, R.G.; Millones, M. Death to Kappa: Birth of Quantity Disagreement and Allocation Disagreement for Accuracy Assessment. *Int. J. Remote Sens.* **2011**, *32*, 4407–4429. [[CrossRef](#)]
81. Huber, M.; Trapp, J. A review of nexrad level ii: Data, distribution, and applications. *J. Terr. Obs.* **2009**, *1*, 4.
82. Bhusal, A.; Ghimire, A.B.; Thakur, B.; Kalra, A. Evaluating the Hydrological Performance of Integrating PCSWMM and NEXRAD Precipitation Product at Different Spatial Scales of Watersheds. *Model. Earth Syst. Environ.* **2023**, *9*, 4251–4264. [[CrossRef](#)]
83. Hamedi, A.; Fuentes, H.R. Comparative Effectiveness and Reliability of NEXRAD Data to Predict Outlet Hydrographs Using the GSSHA and HEC-HMS Hydrologic Models. In Proceedings of the World Environmental and Water Resources Congress 2015, Austin, TX, USA, 17–21 May 2015; pp. 1444–1453. [[CrossRef](#)]
84. Abduljaleel, Y.; Salem, A.; ul Haq, F.; Awad, A.; Amiri, M. Improving Detention Ponds for Effective Stormwater Management and Water Quality Enhancement under Future Climate Change: A Simulation Study Using the PCSWMM Model. *Sci. Rep.* **2023**, *13*, 5555. [[CrossRef](#)]
85. Xiao, H.; Vasconcelos, J.G. Evaluating Curve Number Implementation Alternatives for Peak Flow Predictions in Urbanized Watersheds Using SWMM. *Water* **2023**, *15*, 41. [[CrossRef](#)]
86. Salcedo, S.M.; Suson, P.D.; Milano, A.E.; Ignacio, M.T. Impact of dynamically changing land cover on runoff process: The case of Iligan river basin. In *Remote Sensing for Agriculture, Ecosystems, and Hydrology XVIII*; SPIE: Bellingham, WA, USA, 2016; Volume 9998, pp. 283–297.
87. Chen, X.; Zhang, H.; Chen, W.; Huang, G. Urbanization and Climate Change Impacts on Future Flood Risk in the Pearl River Delta under Shared Socioeconomic Pathways. *Sci. Total Environ.* **2021**, *762*, 143144. [[CrossRef](#)]
88. Gao, J.; Liu, J.; Xu, R.; Pandey, S.; Vankayala Siva, V.S.K.S.; Yu, D. Environmental Pollution Analysis and Impact Study—A Case Study for the Salton Sea in California. *Atmosphere* **2022**, *13*, 914. [[CrossRef](#)]
89. Garg, V.; Nikam, B.R.; Thakur, P.K.; Aggarwal, S.P.; Gupta, P.K.; Srivastav, S.K. Human-Induced Land Use Land Cover Change and Its Impact on Hydrology. *HydroResearch* **2019**, *1*, 48–56. [[CrossRef](#)]
90. Astuti, I.S.; Sahoo, K.; Milewski, A.; Mishra, D.R. Impact of Land Use Land Cover (LULC) Change on Surface Runoff in an Increasingly Urbanized Tropical Watershed. *Water Resour. Manag.* **2019**, *33*, 4087–4103. [[CrossRef](#)]
91. Thakali, R.; Kalra, A.; Ahmad, S.; Qaiser, K. Management of an Urban Stormwater System Using Projected Future Scenarios of Climate Models: A Watershed-Based Modeling Approach. *Open Water* **2018**, *5*, 1.
92. Qin, H.; Li, Z.; Fu, G. The Effects of Low Impact Development on Urban Flooding under Different Rainfall Characteristics. *J. Environ. Manag.* **2013**, *129*, 577–585. [[CrossRef](#)]
93. Ahiablame, L.; Shakya, R. Modeling Flood Reduction Effects of Low Impact Development at a Watershed Scale. *J. Environ. Manag.* **2016**, *171*, 81–91. [[CrossRef](#)]
94. Okwuashi, O.; Ndehedehe, C.E. Integrating Machine Learning with Markov Chain and Cellular Automata Models for Modelling Urban Land Use Change. *Remote Sens. Appl. Soc. Environ.* **2021**, *21*, 100461. [[CrossRef](#)]
95. Zhang, Z.; Hörmann, G.; Huang, J.; Fohrer, N. A Random Forest-Based CA-Markov Model to Examine the Dynamics of Land Use/Cover Change Aided with Remote Sensing and GIS. *Remote Sens.* **2023**, *15*, 2128. [[CrossRef](#)]

**Disclaimer/Publisher’s Note:** The statements, opinions and data contained in all publications are solely those of the individual author(s) and contributor(s) and not of MDPI and/or the editor(s). MDPI and/or the editor(s) disclaim responsibility for any injury to people or property resulting from any ideas, methods, instructions or products referred to in the content.